

1 **Vegetation-induced soil stabilization in coastal area: An example from a natural**
2 **mangrove forest**

3 Zahra Karimi^a, Ehsan Abdi^{a*}, Azade Deljouei^{a,b}, Alessio Cislighi^c, Anoushirvan Shirvany^a, Massimiliano
4 Schwarz^d, Tristram C. Hales^e

5 ^a Department of Forestry and Forest Economics, Faculty of Natural Resources, University of Tehran, Karaj, Iran

6 ^b Department of Forest Engineering, Forest Management Planning and Terrestrial Measurements, Faculty of Silviculture and
7 Forest Engineering, Transilvania University of Brasov, Brasov, Romania

8 ^c Department of Agricultural and Environmental Sciences (DiSAA), University of Milan, Milan, Italy

9 ^d Department of Agronomy, Forestry, and Food Sciences, Bern University of Applied Sciences, Bern, Switzerland

10 ^e School of Earth and Environmental Sciences, Cardiff University, Cardiff, United Kingdom

11 *** Corresponding author: abdie@ut.ac.ir (E. Abdi)**

13 **ORCID of the authors:**

14 - Ehsan Abdi: 0000-0002-3382-7683

15 - Azade Deljouei: 0000-0003-3453-8530

16 - Alessio Cislighi: 0000-0002-4618-818X

17 - Massimiliano Schwarz: 0000-0003-4652-8102

18 - Tristram Hales: 0000-0002-3330-3302

19 **Vegetation-induced soil stabilization in a coastal area: An example from a natural mangrove**
20 **forest**

21 **Abstract**

22 Mangrove forests provide essential ecosystem services in tropical and semitropical regions by supporting
23 their natural regeneration and other biosystem processes, offering livelihood for local communities, and
24 contributing significantly to the natural resources. A systematic analysis on the protective role of mangrove
25 forests and its effect on reducing coastal erosion is rare. Mangroves form a complex ecosystem that increases
26 substrate stabilization and dissipates wave energy favouring the deposition of fine material. This study focuses
27 on assessing the role of the roots of the white mangrove (*Avicennia marina* (Forssk.) Vierh.) in stabilizing the
28 coastline. In a study site located in Southern Iran, a series of field and laboratory measurements of root systems
29 collected from transects perpendicular to the coastline were conducted. Root samples were collected from soil
30 cores at fixed distances from the tree stem in three layers at seaward and landward positions. Moreover, Root
31 tensile tests were conducted to estimate the biomechanical characteristics of roots that provided to the
32 parameters of root reinforcement models. The spatial distribution of root reinforcement and the intrinsic-
33 variability of stabilizing components in relation to horizontal and vertical distances from a tree stem were
34 calculated. Three models of Wu & Waldron (W&W), Fiber Bundle (FBM), and Root Bundle Weibull (RBMw)
35 were applied. The results showed that Root Volume Ratio (RVR) and the number of roots (NoR) decreased with
36 distance from the tree stem. Root tensile forces increased with root diameter. Finally, calculated root
37 reinforcements at 0.75 m distance associated with the highest value while the lowest value was observed at 1.50
38 m from the tree stem with a minor difference between seaward and landward positions. Soil detachment ratio
39 (SDR) as approximately 10% higher at landwards positions than seaward, due to different geomorphological
40 conditions that affected the soil detachment process. The similarity of the values of root reinforcement among
41 root systems at seaward and landward positions may suggest that stem density would not be an important
42 parameter in managing mangrove forests as a coastal protection measure. Yet, RVR at different distances and
43 NoR by increasing significantly with soil depth and being different at seaward and landward positions, could
44 improve their potential role as a nature-based solution for shoreline protection.

45 *Keywords:* *Avicennia marina*, root reinforcement, root system, soil-bioengineering, Soil Detachment Ratio.

46 1. Introduction

47 Coastal erosion is a significant hazard to coastal communities, and the mitigation of such hazard is
48 challenging for many reasons (Dean and Galvin, 1976; Van Rijn, 2011). Nearshore vegetation affects the rate of
49 erosion and deposition of sediments on sandy coasts by moderating the magnitude of tides and waves (Mitra,
50 2020). Vegetation including mangroves and seagrasses, change the hydrodynamics of waves such to dissipate
51 energy and thus, slow down the process of erosion (Feagin et al., 2011; Shepard et al., 2011; Smee, 2019).
52 Reduced wave velocity and turbulence may enhance sedimentation (Anderson and Smith, 2014; Cellone et al.,
53 2016). Roots and rhizomes of nearshore vegetation may reinforce and stabilize coastal sediments. Hence, the
54 propagation of nearshore vegetation may be considered a practical bioengineering method for the protection of
55 coastal zones (Feagin et al., 2019).

56 Mangroves are unique forest ecosystems that reduce the negative impacts of natural soil erosion while
57 maintaining services such as providing construction timber, firewood, charcoal, livestock forage, honey bee
58 habitat and pharmaceutical herbs i.e. saponin, flavonoid, tannins (Rezaii, 1993; Bell and Lovelock, 2013;
59 Thompson et al., 2017). In fact, mangroves mitigate coastal erosion during severe rainstorms by reducing the
60 erosion caused by surge as well as reducing wind erosion (Das and Crépin 2013). They also protect coastal
61 assets by providing bunds that face wave motion (Othman, 1994), stabilize the coastline by reducing wave
62 erosion and enhancing sedimentation (Mazda et al. 2002). A global analysis showed that mangroves function as
63 strong walls that break high waves and prevent water from intruding adjacent lands with high velocity causing
64 excessive soil erosion (Gedan et al., 2011).

65 The south coast of Iran is covered with approximately 20,000 hectares of mangrove forests with patchy
66 distribution. Among such ecosystems, the mangroves of Qeshm Island and Bandar-e Khamir are significant for
67 their vast area (10,000 hectares), also having the highest diversity and largest mangrove-dependent community
68 in the region (Sagheb-Talebi et al., 2014). Two endemic species of Iranian mangroves include the white
69 mangrove (*Avicennia marina* (Forssk.) Vierh.), and the red mangrove (*Rhizophora mucronata* (Poir.)) (Safiari,
70 2003). As mentioned above, developing mangroves are considered an effective bioengineering method to
71 protect soil against erosion as an alternative to conventional engineering methods (soil nailing or concrete
72 piling). Yet ironically in the study area, they themselves are threatened by soil erosion from increasing flood
73 events and forest degradation due to climate change and human interventions (Sagheb-Talebi et al., 2014). Little
74 is known about the relationship between survival rates and biomass production of mangrove species and their
75 impact on coastal erosion.

76 Seafront mangroves species such as *A. marina* have deep, twisted roots that spread like a net and trap soil,
77 keeping it from erosion. Moreover, *A. marina* can tolerate extreme weather conditions and high salinity (Rippey
78 and Rowland, 2004). Root systems control the hydrological and mechanical properties of soil in the rooting
79 depth, favouring stabilization (Gyssels et al., 2005; Hudek et al., 2017; Schwarz et al., 2015; Sidle and Bogaard,
80 2016). Root reinforcement is influenced by root distribution also, the biomechanical characteristics of soil (e.g.,
81 Wu et al., 1979). Such condition is related to botanic, climatic and environmental factors (Hales et al., 2009;
82 Hales & Miniati, 2017) i.e. plant species, stand origin and structure and physical and chemical properties of soil
83 (Bischetti et al., 2005; Deljouei et al., 2020). It has been observed that root reinforcement is systematically
84 dependent on various environmental conditions such as soil moisture (Fan and Su, 2009; Hales et al., 2009),
85 plant functional types (Moresi et al., 2019, Hales, 2018), and plant age (Dazio et al., 2018). In this study,
86 potential environmental controls on mangrove root reinforcement are considered which comprise depth of
87 inundation and wave energy as they actually lack quantitative information.

88 Due to the factors of complex soil-root interactions, heterogenous root distribution and complicated
89 mechanical properties of both soil and roots, assessing root reinforcement remains a challenge (Cohen et al.,
90 2011). Analytical models for soil reinforcement have been developed over the last four decades to support the
91 assessment of hillslope stability as well as to enable appropriate design of soil bioengineering methods
92 (Bischetti et al., 2021; Phillips et al., 2021). Wu & Waldron (W&W) developed a pioneering mechanical model
93 based on the assumption that roots are elastic fibers extending perpendicular to a shear surface and that all roots
94 break at the same time (Wu, 1976; Waldron, 1977). Simplicity of the model led to its world-wide application
95 (Mehtab et al., 2020). On the contrary, roots with different diameters break depending on their individual tensile
96 strength after which the stress is redistributed over the remaining roots. So, the simplified W&W model
97 associates with significant overestimation of root reinforcement (e.g., Operstein and Frydman, 2000; Pollen and
98 Simon, 2005; Docker and Hubble, 2008). Pollen and Simon (2005) developed the Fiber Bundle Model (FBM) as
99 a solution. The model assumes that all roots are parallel and have similar elastic properties. When each root
100 breaks, the load is repetitively redistributed over the remaining roots until all roots (the entire bundle) are
101 broken. Thereofre, the FBM model was found more conservative in estimating soil reinforcement (Bischetti et
102 al., 2009; Mao et al., 2012). An extended version of FBM developed by Schwarz et al. (2013) was the Root
103 Bundle Model weibull (RBMw). RBMw model is based on strain-step loading of a fiber bundle. It integrates a
104 survival function that includes various mechanical properties of roots by implementing empirical relationships
105 along with biomechanical and geometric characteristics of roots, and root distribution in soil. Compared to the

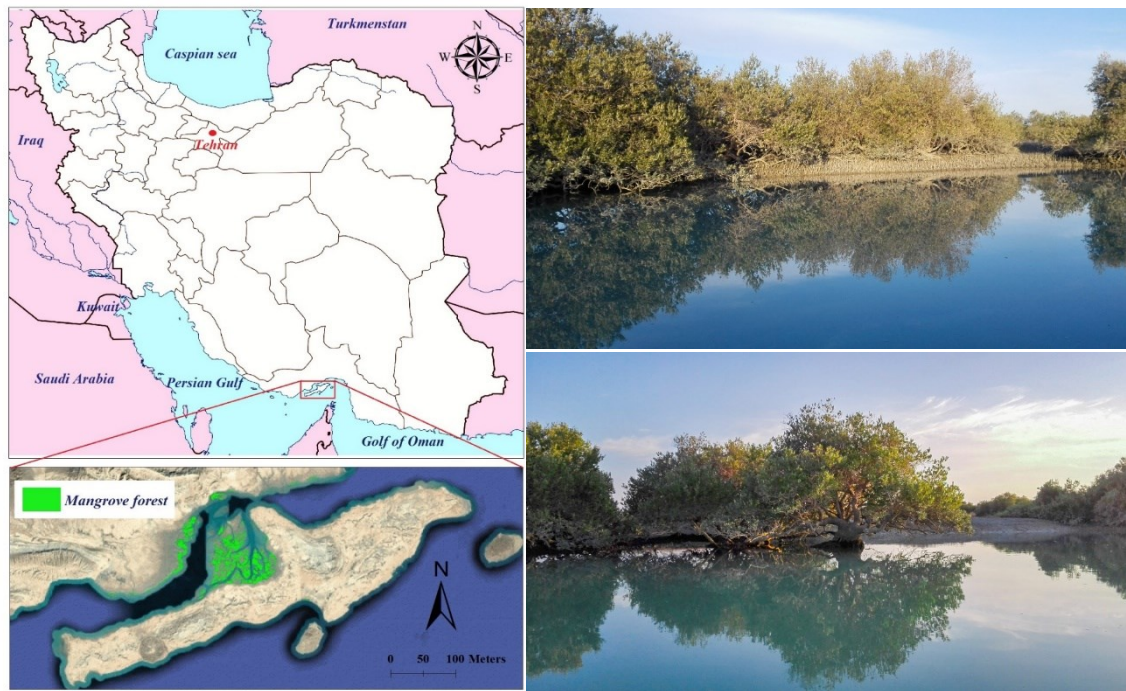
106 W&W model, RBMw requires more parameters, although it predicts more accurate results (Schwarz et al.,
107 2013).

108 This study investigates root characteristics and their mechanical behavior according to distances from the
109 stem at seaward and landward positions by applying different root-reinforcement models. Current knowledge of
110 the underground parts of the mangrove ecosystems is minute. While only few studies have shown that mangrove
111 species can protect shallower soil against coastal erosion (Thampanya et al., 2006; Van Tang et al., 2020), no
112 study has quantified soil reinforcement provided by mangrove roots. In particular, a systematic understanding of
113 Root Volume Ratio (RVR), Number of Roots (NoR), Root Length Density (RLD), and root resistance of
114 mangroves is obtained as measuring underground processes is very difficult, especially at regular flooding areas.
115 Hence, this study aims to: (i) investigate root characteristics and distribution (RVR, NoR, and RLD), (ii)
116 measure the mechanical properties of roots (i.e., root tensile), (iii) compare estimations of the root reinforcement
117 models of W&W, FBM, and RBMw and finally (iv) underline the accuracy of different methods by comparing
118 their estimations. Finally, the role of mangrove forests in protecting coastal erosion is verified by analyzing the
119 results.

120 **2. Material and methods**

121 *2.1. Study site*

122 Hara Biosphere Reserve situated between the southern coastline of the main body of Iran and the northern
123 coastline of Qeshm Island is chosen as the study site. The study focuses on the mangrove forests of Qeshm
124 Island (as part of Hormozgan province) with an area of ~6750 ha (Fig. 1). With an average annual precipitation
125 lower than 200 mm, the regional climate is dry and classified as subtropical. The evaporation rate is higher than
126 annual precipitation and the annual relative humidity is 64%. Therefore, the mangroves only reach heights of 3-
127 4 m. The soil (pH=7.67) has a very fine texture and consists of loam, sand, and clay. When saturated, it can
128 retain 56.8% of moisture (Mohammadizadeh et al., 2009). Electrical conductivity (EC) of the saturated soil and
129 water salinity is reported 63.5 dS/m and 37.5 to 38.5 ppt, respectively (Khodadadi-Jokari, 2003). Atmospheric
130 temperature varies from 10°C to 45°C, and the water temperature fluctuates as much as 20°C between summer
131 and winter. Tidal waves vary between 4.6 m (during fall and spring seasons) and 0.3 m (during winter and
132 summer seasons), respectively. During the high-tide season, the mangrove trees are submerged up to their
133 crowns.



134

135

Fig. 1. Location of mangrove forest in Qeshm Island

136

2.2. Measurements of root distribution and biomechanical properties

137

138

139

140

141

142

143

144

145

146

147

148

The underground biomass and root distribution were measured using the core sampling method for 10 *A. marina* trees (Montagnoli et al., 2012; Fortier et al., 2013; Berhongaray et al., 2015). Trees with the mean diameter of 0.25 m at breast height (DBH) were sampled by a hand-driven corer of 0.10 m diameter, 0.10 m length and 0.0079 m³ volume. Samples were collected along transects perpendicular to the coastline at fixed distances of 0.75 m, 1.00 m, and 1.50 m from the tree stem at both seaward and landward positions and at 0.00-0.10 m (top layer), 0.10-0.20 m (midlayer), and 0.20-0.30 m (bottom layer) depths. Root biomass was collected in the field by sieving (0.002 m mesh size). Root diameters were measured in the field using a digital caliper. The final biomass was determined by washing and drying roots in a 70°C oven while weighing them until reaching a constant weight. RVR (in m³ m⁻³), is the total volume of roots in a particular soil volume (Ni et al., 2018); NoR (dimensionless) is the, Number of Roots (as a function of diameter); and RLD (Root Length Density, in m⁻²) is the mean value of root length per sample soil volume which calculated. In addition, tensile tests were carried out on root samples collected around the tree stem.

149

2.3. Tensile measurements

150

151

Undamaged root specimens collected from each core were washed, sprayed with 15% alcohol, kept in plastics, and retained at 5°C until the tensile test was carried out (Chiaradia et al., 2016; Abdi and Deljouei,

152 2019). Within three days after the root sampling, tensile tests were conducted on fresh roots. Roots with the
 153 length of 0.15 m were placed in the clamps of the Universal Testing Machine (SANTAM Co./SMT-5, Tehran,
 154 Iran), and mechanical tests were conducted at a steady 10 mm min⁻¹ speed until rupture. Only specimens that
 155 broke near the middle of the root segment were considered (Ji et al., 2012).

156 The main results of the tensile tests fit the relationships between the root diameter and biomechanical
 157 properties as follows:

$$158 \quad F_{\max} = F_0 \phi^\xi, \quad (1)$$

$$159 \quad E = E_0 \phi^\beta, \quad (2)$$

160 where F_{\max} is root tensile resistance (N), E is root elasticity (MPa), F_0 and E_0 are constant coefficients (N and
 161 MPa, respectively), ξ and β are exponents (dimensionless), and ϕ is root diameter in mm.

162 2.4. Root reinforcement models

163 In this study, root reinforcement (C_r in N m⁻²) assessment was conducted using three models: W&W, FBM
 164 and RBMw.

165 The W&W (Wu et al. 1988) model calculates root reinforcement assuming that all roots break at the same
 166 time and thus, each root contributes individually to the tensile resistance as follows:

$$167 \quad C_r = k' \sum_{n=1}^N \frac{4F_{\max,n}}{\phi_n^2 \pi} \cdot RAR_n, \quad (3)$$

168 where k' is a coefficient of 1.2 (Wu, 1976), N is the number of classes of root diameter and RAR_n is the root
 169 area ratio (the ratio between soil area covered by roots and the entire soil profile, in m² m⁻²) for the n -th class.

170 The FBM (Pollen and Simon, 2005) model applies load to the bundle of fibers and distributes it evenly over
 171 each root as a function of the number of roots in the bundle. The load is redistributed after each root breaks. This
 172 model assumes that the roots are perpendicular to the shear surface and the distribution of stress across the roots
 173 is uniform (Schwarz et al., 2010b). The shortcoming of this method is that the heterogeneous distribution of load
 174 due to different stiffness root diameter classes are not considered (Schwarz et al., 2010b). The formulation of
 175 FBM is as follows:

$$176 \quad C_r = \max\left(\frac{4F_{\max,j}}{\phi_j^2 \pi} \cdot RAR_j \cdot j\right), \quad (4)$$

177 where j is the weakest root which is still intact upon loading of the root bundle, RAR_j is the RAR of the root
 178 j .

179 The RBMw (Schwarz et al., 2013) model, is a strain-step fiber bundle model that considers the failure
 180 probability of roots due to its variable mechanical properties. RBMw simulates force-displacement behavior of a
 181 root bundle based on a distribution of root diameter and a series of power-distributed relationships between
 182 biomechanical properties (Eqs. 1 and 2) and ϕ , and between root length (L in mm) and ϕ (Eq. 5).

$$183 \quad L = L_0 \phi^\alpha \quad , \quad (5)$$

184 where L_0 is a constant coefficient (in mm), and α is an exponent value (dimensionless).

185 C_r is calculated by summing up the force contributions F (in N) for each root multiplied by the Weibull
 186 survival function S , as follows:

$$187 \quad C_r = \sum_{i=1}^N F(\phi_i, \Delta x) S(\Delta x^*) \quad , \quad (6)$$

188 where Δx is the displacement unit in mm and S is a function of the normalized displacement Δx^* . The
 189 following equation calculates $S(\Delta x^*)$:

$$190 \quad S(\Delta x^*) = \exp \left[- \left(\frac{\Delta x^*}{\lambda} \right)^\omega \right] \quad , \quad (7)$$

191 where λ and ω (dimensionless) are scale and shape Weibull parameters, respectively.

192 The ratio between displacement is estimated by each tensile test and the corresponding displacement values
 193 are calculated using fitted values of tensile forces:

$$194 \quad F(\phi_i, \Delta x) = \frac{\pi E_0}{4L_0} \phi_i^{2+\beta-\alpha} \quad F(\phi_i, \Delta x) < F_{max}(\phi_i) \quad (8)$$

195 In this research, all input parameters (F_0 , E_0 , L_0 , ζ , β , and α) were calculated from tensile tests.

196 2.5. Soil detachment ratio

197 Erosion of estuaries that contain mangroves occurs primarily through the action of waves and tides that
 198 apply shear stress on surface sediments (Nguyen & Luong, 2019). Rates of soil detachment depend on the
 199 magnitude of the shear stress applied, and is resisted by the cohesion of the sediment as well as the subsurface

200 root system. *A. marina* roots develop a fibrous mat in shallow subsurface (Baylis, 1950) that adds support
 201 against such flow erosion. Without a mangrove specific erosion rule, soil detachment rates (SDR) were
 202 calculated using a standard equation developed for terrestrial root systems that are subject to concentrated flow
 203 erosion. SDR was calculated as

$$204 \quad SDR = \exp^{(-b \times RD)} \exp^{(-c \times RD \times \phi)} \quad , \quad (9)$$

205 where b and c are constant parameters with 2.15 and -0.13 values, respectively (Vannoppen et al., 2017). We
 206 acknowledge the lack of data on the parameter values for mangrove, hence they are considered same as the
 207 average values for roots penetrating a silty loam (Vannoppen et al., 2017). Root Density (RD) is calculated in kg
 208 m^{-3} as follows:

$$209 \quad RD = \frac{M_D}{V} \quad , \quad (10)$$

210 where M_D (kg) is the dry living root mass and V (m^3) is the volume of soil sample (i.e., 0.00785 m^3). SDR
 211 values range between 0 and 1. Conversely, higher values indicate the less efficiency of roots in reducing soil
 212 erosion.

213 2.6. Statistical analysis

214 The normality and homogeneity of data were checked before performing the analysis. Since the data did not
 215 fit a normal distribution, a log transformation was applied. Mean values of RVR, NoR, RLD, and C_r for seaward
 216 and landward positions were compared by ANOVA among three distances from tree stems. Additionally, an
 217 ANOVA test was applied to compare root reinforcement models (i.e., W&W, FBM, and RBMw). It was also
 218 possible to assess variations in tensile force since the roots were collected from both sides of the tree samples.
 219 Analysis of covariance (ANCOVA) was used to determine whether the position of the samples affected root
 220 tensile forces or not. Root diameter was considered as a covariate factor based on the preliminary use of
 221 ANCOVA, which yielded the lowest residuals. Confidence intervals were established at 0.05 probability levels.

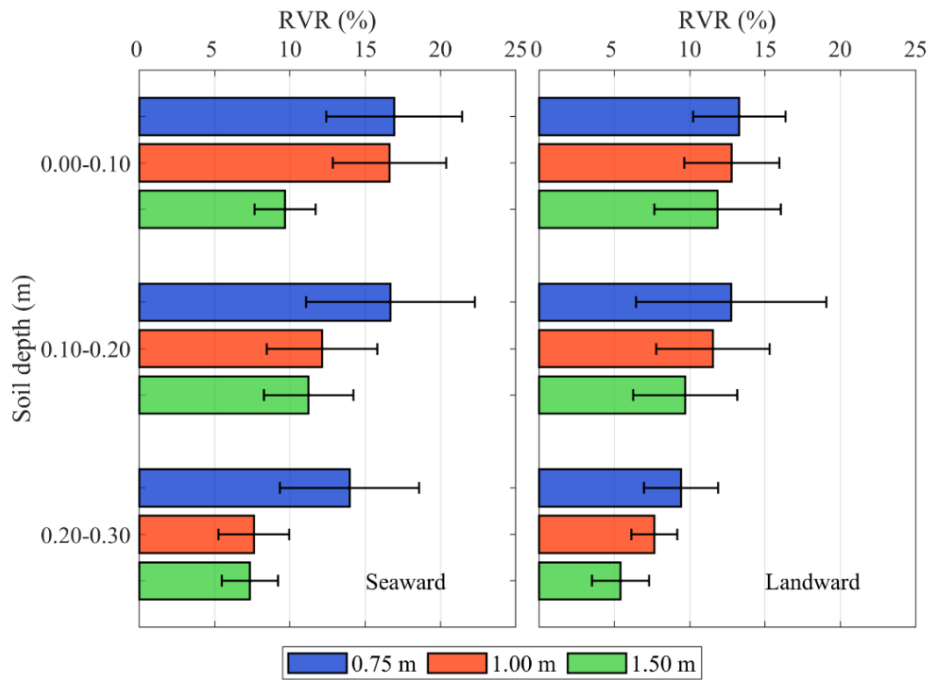
222 3. Results

223 3.1. Root distribution

224 3.1.1. Root Volume Ratio

225 As indicated in Figure 2, RVR values generally decreased with soil depth at both seaward and landward
 226 positions. They decreased systematically moving away from the tree stem (from 0.75 m to 1.50 m distance),

227 with relatively higher ratios at seaward positions. The ANOVA test showed that mean values of RVR at
 228 different distances from tree stems were significantly different ($F=5.49$, $p<0.05$) i.e. significantly lower at 1.50
 229 m distance than the two other. At similar positions in terms of distance and depth, corresponding RVR
 230 measurements at seaward and landward positions were not significantly different ($p>0.05$; Fig. 2).



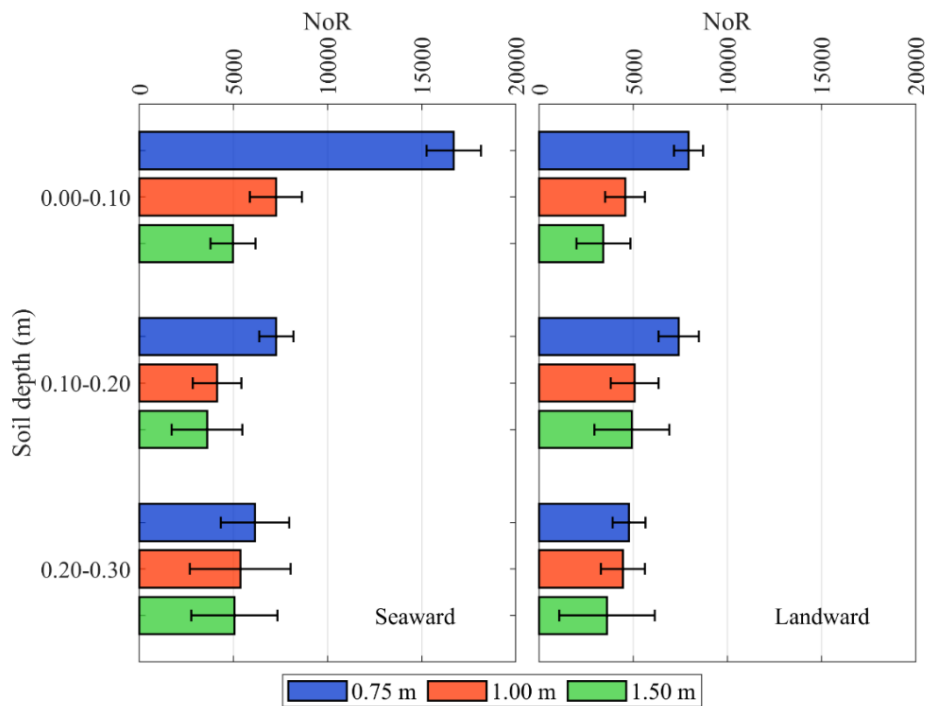
231

232 **Fig. 2.** Variability of RVR values at different positions (distance from tree stem and soil depth) at seaward and
 233 landward positions

234 3.1.2. Number of roots

235 Highest NoR values were observed near the core of the tree stem yet, they were more dense at seaward than
 236 landward positions (Fig. 3). As illustrated, NoR generally reduced with soil depth at both sides (landward and
 237 seaward). Regarding seaward positions, average NoR values in the top and bottom layers of soil at 0.75 m from
 238 the stem were 16694 and 4982, respectively. Corresponding values reduced to 7277 and 3603 at 1.00 m, also
 239 6142 and 5061 at 1.50 m distance. Landward NoR values were generally lower. The average values obtained for
 240 the top and bottom layers were 7933 and 3414 at 0.75 m distance, 7413 and 4928 at 1.00 m distance and finally,
 241 4775 and 3603 at 1.50 m distance, respectively. While 45% percent of roots were found in the top layer, only
 242 25% were observed in the bottom layer. In cores taken from near tree stem positions, the declining rate of NoR
 243 with soil depth was sharper in comparison to farther distances (Fig. 3). Although root diameters varied from 0.1
 244 mm to 17.2 mm at seaward positions, the majority of roots (99.4%) were very fine (within the <1 mm diameter

245 class), regardless of the distance from the stem. Less than 0.4% of the roots were 1-2 mm in diameter and about
 246 0.2% were just greater than 2 mm. At landward positions, roots diameters ranged from 0.01 to 20.93 mm of
 247 which 98.2% were less than 1 mm. 1.6% of the roots were 1-2 mm in diameter and 0.2% were just thicker.
 248 Comparing the NoR between seaward and landward positions revealed no significant statistical difference
 249 between corresponding distances from tree stems and soil depths ($p>0.05$; Fig. 3).

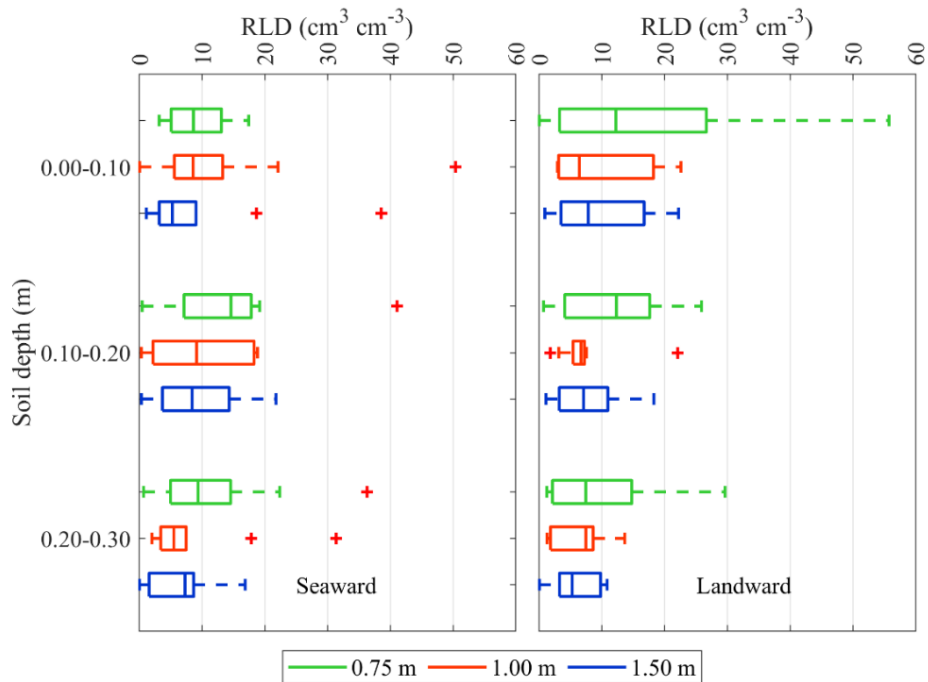


250

251 **Fig. 3.** Number of Roots at the distances of 0.75 m, 1.00 m, and 1.50 m from the tree stem for both seaward and
 252 landward positions

253 *3.1.3. Root Length Density*

254 As shown in Fig. 4, the measurements of RLD were consistent at seaward and landward positions. In most
 255 cases, the RLD value at seaward position was higher than its corresponding value at landward position. The top
 256 layer at 0.75 m and 1.50 m distances and the mid layer at 1.00 m distance were exceptions. However in all
 257 cases, the mean value of RLD at corresponding positions were not significantly different ($p>0.05$; Fig. 4).
 258 Furthermore, RLD values were not significantly different ($p>0.05$) at any specific depth of a the same distance
 259 at both sides. In addition in different soil depths at a certain distance RLD values were quite similar ($p>0.05$;
 260 Fig. 4).



261

262 **Fig. 4.** Values of RLD at different distances from the tree stem and different soil depths at seaward and

263

landward positions

264 *3.2. Root tensile test*

265

266

267

268

269

270

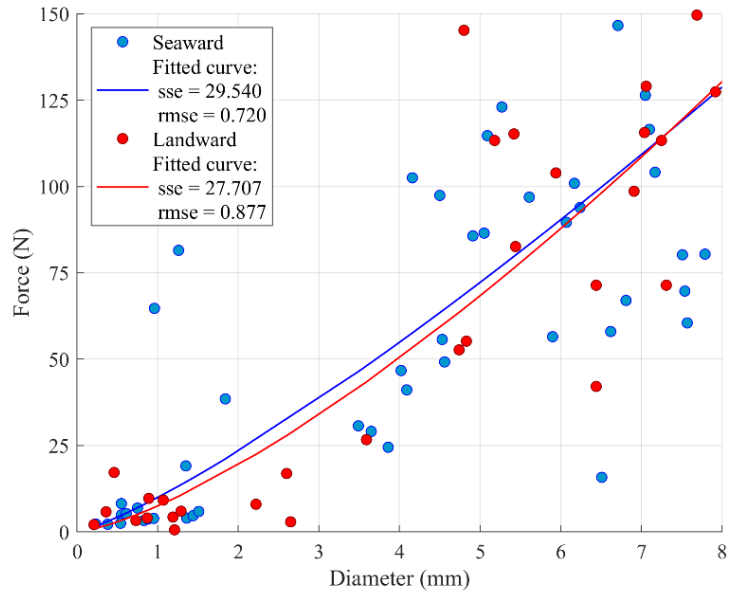
271

272

273

274

Laboratory tests were conducted on 59 sample roots from seaward positions and 39 sample roots from landward positions with diameters ranging from 0.21 mm to 8.85 mm. The relationship between root diameters and tensile forces is shown in Figure 5. As shown, failure forces increased with root diameters at both directions (seaward and landward). Results indicated that maximum tensile forces ranged from 2.2 N to 226.6 N at seaward positions (where root diameters varied between 0.23 and 8.76 mm), and from 0.6 N to 287.9 N at landward positions (where root diameter varied between 0.21 and 8.85 mm). Failure forces were not significantly different (ANCOVA, $F = 0.58$; $p > 0.05$) in the two directions whereas root diameter, as a covariate parameter, was significant ($F = 114.2$; $p < 0.05$). ANCOVA verified similarities between the curves of force against root diameter at different distances, making it possible to aggregate data and achieve a single force vs. root diameter curve.



275

276

Fig. 5. Root diameter-tensile force relation at seaward and landward positions

277

3.3. Root reinforcement models

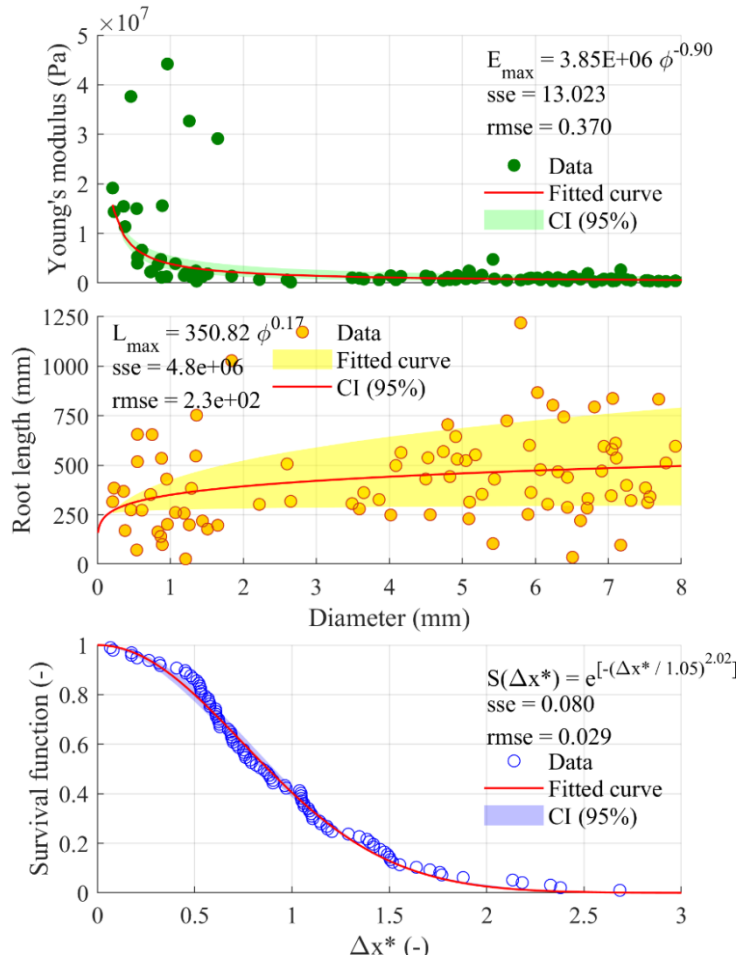
278

3.3.1. Input parameters

279

All three models require the relationship between tensile force and root diameters (Eq. 1). The results of root tensile tests indicated strong correlations between the mechanical and geometrical characteristics of roots and root diameters through a power-law regression line. In particular, an appropriate fit was obtained for the ultimate resistant force and Young's modulus (Fig. 6). The results of tensile tests fitted a survival function with robust fitting performance (Fig. 6).

283

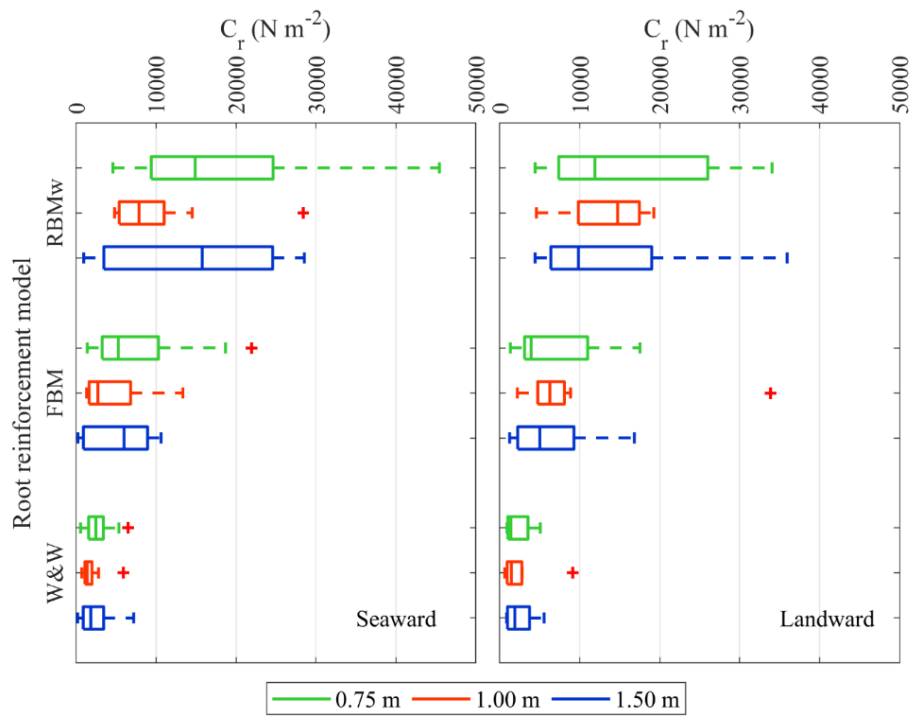


284
285 **Fig. 6.** Calibration of input parameters of the root reinforcement models

286 3.3.2. Assessing root reinforcement using different root reinforcement models

287 In all three models, C_r decreased with distance from the tree stem. The average values of C_r at 0.75 m
 288 distance seaward were 9710.55 N m^{-2} for W&W, 3468.90 N m^{-2} for FBM, and 1880.62 N m^{-2} for RBMw (Fig.
 289 7). Also at 1.50 m distance seaward, C_r values of 6240.85 N m^{-2} , 3245.70 N m^{-2} , and 1604.88 N m^{-2} were
 290 obtained for W&W, FBM, and RBMw models, respectively (Fig. 7). The graph shows that C_r values reached
 291 4271.33 N m^{-2} for W&W, 3251.80 N m^{-2} for FBM, and 1130.36 N m^{-2} for RBMw at 0.75 m distance landward.
 292 C_r values of W&W, FBM, and RBMw models at 1.50 m distance landward were 3711.35, 1947.40, and 1763.39
 293 N m^{-2} , respectively. Therefore, the estimated value of C_r by RBMw at the distance of 1.50 m was 9.9% higher at
 294 the landward than seaward position (Fig. 7). For all models, the highest Coefficient of Variation (CV) was
 295 obtained in the top layer landward (Table 1). Except for the midlayer seaward, the RBMw model estimated the
 296 lowest CV among all root reinforcement models (Table 1). The ANOVA test showed that root reinforcement
 297 estimated by W&W, FBM, and RBMw models at different distances were not statistically significant at seaward

298 and landward positions ($p>0.05$; Fig. 7). Also, statistical analysis showed that root reinforcement in each model
 299 and at each direction did not vary significantly among distances ($p>0.05$; Fig. 7).



300

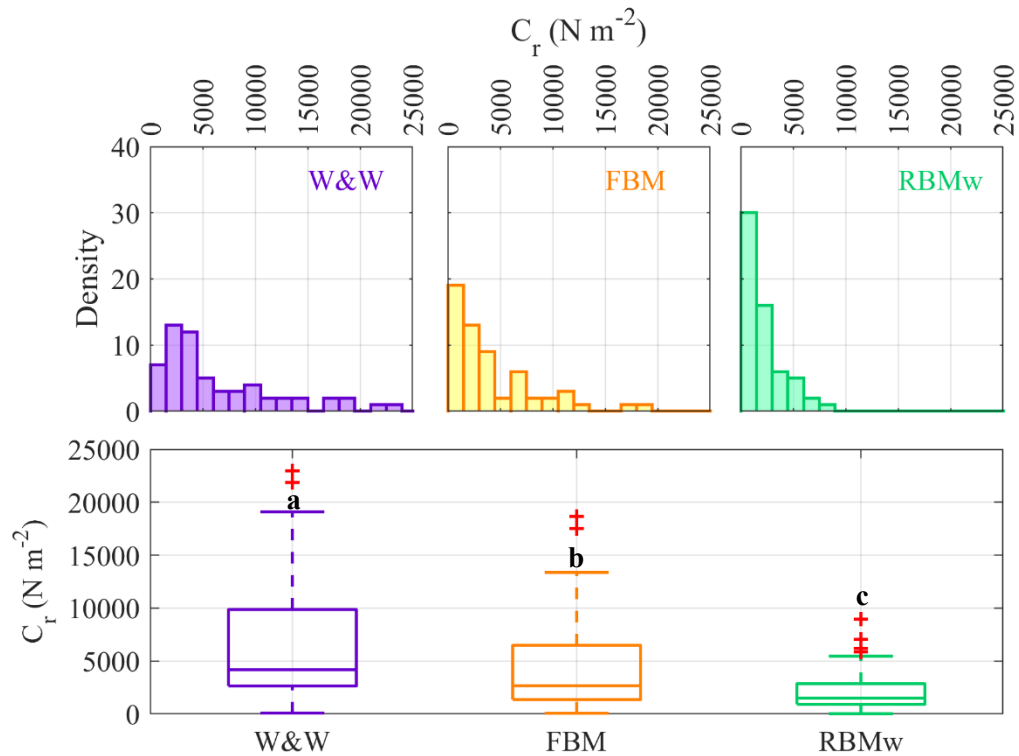
301 **Fig. 7.** Root reinforcement (C_r) of Wu & Waldron Model (W&W), Fiber Bundle Model (FBM), and Root
 302 Bundle Model-Weibull (RBMw) at different distances of landward and seaward directions. Bars denote standard
 303 error (\pm SE).

304 **Table 1** Coefficient of variation (CV) of root reinforcement values estimated by Wu & Waldron Model, Fiber
 305 Bundle Model, and Root Bundle Model-Weibull at different distances of landward and seaward directions

Position	Depth (m)	CV		
		W&W	FBM	RBMw
Seaward	0.00-0.10	0.74	0.94	0.69
	0.10-0.20	1.13	1.35	0.85
	0.20-0.30	0.81	0.83	0.96
Landward	0.00-0.10	0.96	1.02	0.78
	0.10-0.20	1.69	1.68	1.14
	0.20-0.30	0.85	0.87	0.77

306 Results showed that all models resulted in significant differences among root reinforcement values, ranging
 307 from 31 $N m^{-2}$ to 34000 $N m^{-2}$ (Fig. 8). More specifically, C_r ranged from 80 to 52000 $N m^{-2}$ for W&W, 70 to
 308 34000 $N m^{-2}$ for FBM, and from 31 to 9000 $N m^{-2}$ for RBMw (Fig. 8). W&W provided the highest and RBM
 309 provided the lowest values (more conservative and thus, appropriate to apply).

310 The results of ANOVA tests showed that among all models, the C_r estimated by W&W was significantly the
 311 highest ($F= 11.61$, $p<0.05$; Fig. 8) and that of the RBMw was significantly the lowest (Fig. 8).



312
 313 **Fig. 8.** Comparison of root reinforcement of Wu & Waldron model, fiber bundle model, and root bundle model-
 314 Weibull. Boxes with the different lowercase letters are significantly different ($p<0.05$).

315 *3.4. Soil detachment ratio*

316 According to Table 2 at seaward positions, the mean value of SDR ranged from 0.31 (at 0.75 m distance, top
 317 layer and at 1.00 m distance, midlayer) to 0.49 (at 1.50 m distance, midlayer). At landward positions, the values
 318 varied between 0.39 and 0.48 at 0.75 m distance, midlayer and 1.50 m distance, bottom layer soil depth,
 319 respectively. Overall, mean SDR values were higher at landward positions (0.42 vs. 0.38, respectively).

320 **Table 2** Soil detachment ratio (SDR) values at different distances and different soil depths at seaward and
 321 landward positions

Position	Distance (m)	Depth (m)	SDR			
			Min	Mean	Max	SE (\pm)
Seaward	0.75	0.00-0.10	0.001	0.31	0.56	0.06
		0.10-0.20	0.006	0.34	0.77	0.06
		0.20-0.30	0.001	0.32	0.56	0.06
	1.00	0.00-0.10	8.6×10^{-5}	0.36	0.62	0.06
		0.10-0.20	0.117	0.31	0.53	0.04

		0.20-0.30	0.299	0.48	0.68	0.04
		0.00-0.10	0.020	0.39	0.91	0.07
	1.50	0.10-0.20	0.187	0.46	0.89	0.07
		0.20-0.30	0.318	0.49	0.70	0.04
	Mean		8.6×10⁻⁵	0.38	0.91	0.02
		0.00-0.10	0.092	0.40	0.72	0.06
	0.75	0.10-0.20	0.117	0.39	0.63	0.05
		0.20-0.30	0.181	0.41	0.72	0.06
		0.00-0.10	0.086	0.40	0.81	0.07
Landward	1.00	0.10-0.20	0.120	0.40	0.66	0.05
		0.20-0.30	0.205	0.44	0.64	0.04
		0.00-0.10	0.117	0.46	0.78	0.06
	1.50	0.10-0.20	0.046	0.38	0.92	0.08
		0.20-0.30	0.114	0.48	0.88	0.07
	Mean		0.046	0.42	0.92	0.02

322

323 4. Discussion

324 As resulted in previous studies, root density dramatically decreases with soil depth (Stokes et al., 2009;
325 Moresi et al., 2019; Abdi and Deljouei, 2019). Decreasing root density with soil depth has been correlated with
326 less nutrient availability, less soil aeration, and higher presence of compact layers (Moresi et al., 2019; Abdi and
327 Deljouei, 2019). Similar investigations were carried out on *Alnus subcordata*, *Acer velutinum*, and *Parrotia*
328 *persica* native and pioneer species of the Hyrcanian ecoregion to identify root density patterns. Results show
329 that patterns were similar to *A. marina* in all layers and not significantly different (Abdi and Deljouei, 2019).
330 Furthermore, in several studies, decreasing root densities in the horizontal direction were investigated in relation
331 to distance from the stem, tree diameter, species, and micro-topography (Genet et al., 2005; Schwarz et al.,
332 2010a; Ji et al., 2012; Dazio et al., 2018; Bordoni et al., 2020; Cislighi et al., 2021). Spatial variability of root
333 expansion (i.e., vertical and horizontal) depends on many variables including climate, local soil, land use
334 management as well as associated vegetation communities (Sidle and Ochiai, 2006). The total number of roots
335 in this study was completely different than other researches, taking into account the species, distance from the
336 stem, and numbers of very fine roots which could be explained by the greater concentration of soil nutrients near
337 the soil surface (Castañeda-Moya et al., 2011). Specific environmental conditions of Iranian mangrove due to
338 permanent tide stress may justify the unusual mass and deeper root system. In this study, fine roots were the
339 main part of the total rootstock, providing 98.2%-99.4% of standing root biomass. The primary function of fine
340 roots in absorbing water and soil nutrients was clarified (Sanchez 2005), especially during early root
341 development. In contrast, coarse roots represented a higher fraction of total root biomass in Florida and Mexico

342 (Castañeda-Moya et al., 2011; Adame et al., 2014). The results of this study showed that root densities were not
343 significantly different at seaward and landward positions. Chiatante et al. (2003) stated that asymmetric cross-
344 sections cause variations in mechanical characteristics of roots. Furthermore, Di Iorio et al. (2005) reported that
345 larger root sections could be resulted from higher loading stresses. Consequently, results may support the
346 hypothesis that the roots of the trees that were investigated by mechanical stresses had the same condition
347 seawards and landwards. Morphoplasticity (Marler and Discekici, 1997) or phenotypic plasticity (Ganatsas and
348 Spanos, 2005) describes the ability of plants to adapt with environmental conditions. The similarity between the
349 number of roots in corresponding seaward and landward positions could indicate that the plant reacts to stress by
350 thickening its roots instead of increasing its root number.

351 RLD is a root characteristic specified as either root length per unit of soil volume or root length per unit of
352 soil surface (Stokes et al., 2009). RLD is often used as an indicator for stabilizing slopes and soil that is explored
353 by a root system in search of nutrients and soil water (Aziz et al., 2017; Bordoloi and Ng, 2020) since it better
354 reflects the quantity and structural aspects of roots (Yang et al., 2018; Hamidifar et al., 2018; Lobmann et al.,
355 2020). Its value decreases with soil depth due to the higher nutrient level in top layer of soil (Pandey et al.,
356 2000; Hoad et al., 2001; Bayala et al., 2002, 2004). The erodibility of topsoil is known to be dramatically less as
357 the density of root length is higher (e.g., Mamo and Bubenzer, 2001a, b; De Baets et al., 2006; Knapen et al.,
358 2007; Osman and Barakbah, 2011). RLD reduction with distances from tree trunks was evident in all depths.
359 The rate suggests potential competition directly under the tree crowns for water and nutrients (Odhiambo et al.,
360 2001; Bayala et al., 2004). The most contributive factor of soil aggregate is RLD such that lower RLD in further
361 distances is expected to reduce soil stabilization more (Demenois et al., 2017). From a soil bioengineering
362 perspective, RLD is defined as a mechanical soil reinforcement method (Osman and Barakbah, 2011). High
363 RLD values imply a higher cross-section area of roots on a potential shear surface per unit of soil surface in
364 terms and thus, higher mechanical reinforcement (Ghestem et al., 2014; Boldrin et al., 2017).

365 The relation between root diameter and tensile force was found significant which complied with the results
366 of other studies in which the tensile force strongly depended on root size (Genet et al., 2010; Boldrin et al.,
367 2017; Abdi and Deljouei, 2019; Deljouei et al., 2020). Therefore, hence it is necessary to take the root diameter
368 into account as a covariate for root tensile force analysis (Vergani et al., 2012; Moresi et al., 2019; Abdi et al.,
369 2019). The relationship between root diameter and tensile force was investigated as a positive power-law
370 function in previous studies (Bischetti et al., 2005; Genet et al., 2010; Vergani et al., 2012). Different cellulose
371 to lignin ratios justified this relationship, with smaller roots having higher cellulose:lignin (Genet et al., 2005).

372 Such result were also due to the chemical composition of root tissues; root tensile forces had a significantly
373 negative correlation with cellulose and holocellulose amounts and a significantly positive correlation with lignin
374 and its ratio to cellulose (Ye et al., 2017).

375 According to the results, the estimates of root reinforcement by the W&W model significantly varied with
376 those of FBM and RBMw models. In literature, the value of k' coefficient used in the W&W model depended
377 strongly on the root bending angle as wells as the effective internal friction angle of soil (Wu, 1995; Danjon et
378 al., 2008). Hence, it was suggested to use the correction factor k'' instead. Most researchers quantified its value
379 from 0.4 (Preti, 2006) to much lower values in order to correct the overestimation of the W&W (Operstein and
380 Frydman, 2000; Docker and Hubble, 2008; Cislighi, 2018; Deljouei, 2019). Bischetti et al. (2009) compared
381 W&W and FBM models, and showed that k'' coefficient was correlated with the number of roots. For a density
382 smaller than 400 m⁻² roots, a greater than 0.5 value may be assumed for k'' (Bischetti et al., 2009). Cislighi
383 (2018) suggested that various combinations of k'' should be used with 0.3 being most appropriate. This study
384 suggests that considering k'' of 0.3 for the W&W model provides the closest estimation to RBMw-values.
385 Deljouei (2019) identified k'' be 0.3 for small *Carpinus betulus* trees (0.75-0.325 m DBH), 0.4 for medium trees
386 (0.326-0.575 m DBH), and 0.1 for large trees (0.576-0.825 m DBH) for most accurate estimations in the W&W
387 model. Moreover, the k'' coefficient was estimated 0.3 for small and medium trees of *Fagus orientalis*, and 0.2
388 for large trees. Among root reinforcement models, W&W is the simplest as it requires a limited number of input
389 parameters (i.e., RAR and tensile force-root diameter curves). However, it is necessary to estimate the C_r value
390 more accurately and avoid overestimation, therefore FBM will improve the estimations of root reinforcement
391 ratios of other models and overcome the hypothesis of simultaneous root-breaking. Several authors suggested
392 that FBM provides encouraging estimates using available parameters, whereas RBMw requires many input
393 parameters for an accurate and reliable estimation of the mechanical characteristics of a root system (Schwarz et
394 al., 2013). In comparison to FBM, RBMw enables a less simplified breaking process for the bundle of roots by
395 considering a progressive failure of roots due to their heterogeneous distribution. The main variable influencing
396 root reinforcement estimations by W&W, FBM, and RBMw models is root diameter distribution (Vergani,
397 2013). Different studies, field observations and laboratory tests show that the mechanical properties of roots
398 highly vary even within the same diameter class. Such quality is due to the anatomy and geometry of roots,
399 resulting in different failure forces and displacements which is considered in the RBMw model by fitting in the
400 survival function parameter ω .

401 SDR values showed that soil erosion reduction due to the presence of roots in landward position were circa
402 10% higher than seaward position. The finding is useful in conserving or restoring mangrove forests at seaward
403 positions and provide nature-based shoreline protection as shoreline protection in mangrove ecosystems are
404 mostly needed in this direction. Although the soil stabilizing and erosion reduction effect of tree roots for soil in
405 various forest ecosystems are well-known (e.g., Abdi and Deljouei, 2019; Abdi et al., 2019), the functional role
406 of mangrove forests in reducing erosion at seaward and landward directions (i.e., landward and seaward
407 positions) has not been described yet. In line with the results of this research, Gou et al. (2020) showed that
408 difference in SDR values may be related to different geomorphological conditions that affected the soil
409 detachment process (De Baets et al., 2007; Li et al., 2015). The study also revealed indirectly that different
410 conditions should be seriously considered in erosion control revegetation efforts.

411 Compared with the simplest model (W&W), the RBMw enables a comprehensive evaluation of root
412 reinforcement with only few additional parameters and performs reasonably accurate predictions. Results of this
413 study provide helpful information and tools for quantifying root reinforcement as a crucial factor for
414 understanding numerous hydrologic and earth surface processes. Our results highlighted that the RBMw model
415 estimations for root reinforcement were more conservative in which the lowest quantities among the three
416 adopted models were obtained. In order to apply the results of this study to other mangrove areas, the RBMw
417 estimation is recommended among other soil erosion prediction models. Finally, the significant role of *A.*
418 *marina* in reducing soil erosion and conserving nutrient levels in the mangrove forest were evident in this
419 research.

420 **5. Conclusions**

421 This research estimated the effect of the most significant mangrove species (i.e., *Avicennia marina*) at
422 present time in Iran on soil stability. RVR, RLD, RD, and SDR were calculated at various soil depths with
423 respect to the biomechanical characteristics of roots. Study results showed that root reinforcement greatly
424 enhanced soil stability, highlighting the effectiveness of white mangrove trees in preventing and mitigating soil
425 erosion. Recently, using natural material to increase shear resistance and stiffness of soil has become very
426 common at different places. Geotechnical engineers recognize the role of roots in strengthening soil and the
427 contribution of root resistance in improving soil stability very well. Results indicated that RVR, RLD, root
428 distribution, and biomechanical root characteristics were not significantly different at seaward and landward
429 positions from the tree stem. In contrast, values of all parameters decreased with soil depth and distance from
430 the tree stem. Additionally, it was concluded that quantifying root reinforcement with W&W, FBM, and RBMw

431 models reflected significantly different results through which the W&W overestimated root reinforcement
432 compared to the FBM and RBMw models. The results are particularly important to consider in managing soil
433 erosion in Iran and other similar regions and demonstrate that developing *A. marina* communities can be an
434 effective bioengineering technique for soil stabilization in coastal regions.

435

436 **References**

437 Abdi, E., Deljouei, A., 2019. Seasonal and spatial variability of root reinforcement in three pioneer species of
438 the Hyrcanian forest. *Austrian J. For. Sci.* 136, 175-198.

439 Abdi, E., Saleh, H.R., Majnounian, B., Deljouei, A., 2019. Soil fixation and erosion control by *Haloxylon*
440 *persicum* roots in arid lands, Iran. *J. Arid Land* 11(1), 86-96.

441 Aburto-Oropeza, O., Ezcurra, E., Danemann, G., Valdez, V., Murray, J., Sala, E., 2008. Mangroves in the Gulf
442 of California increase fishery yields. *Proc. Nat. Acad. Sci.* 105(30), 10456-10459.

443 Adame, M.F., Teutli, C., Santini, N.S., Caamal, J.P., Zaldívar-Jiménez, A., Hernández, R., Herrera-Silveira, J.A.,
444 2014. Root biomass and production of mangroves surrounding a karstic oligotrophic coastal lagoon.
445 *Wetlands* 34(3), 479–488.

446 Anderson, M.E., Smith, J.M., 2014. Wave attenuation by flexible, idealized salt marsh vegetation. *Coastal Eng.*
447 83, 82-92.

448 Andreoli, A., Chiaradia, E. A., Cislighi, A., Bischetti, G. B., Comiti, F., 2020. Roots reinforcement by riparian
449 trees in restored rivers. *Geomorphology*, 370, 107389.

450 Aziz, M.M., Palta, J.A., Siddique, K.H., Sadras, V.O., 2017. Five decades of selection for yield reduced root
451 length density and increased nitrogen uptake per unit root length in Australian wheat varieties. *Plant Soil*
452 413(1-2), 181-192.

453 Bayala, J., Teklehaimanot, Z., Ouedraogo, S., 2004. Fine root distribution of pruned trees and associated crops
454 in a parkland system in Burkina Faso. *Agroforestry Sys.* 60, 13-26.

455 Bayala, J., Teklehaimanot, Z., Ouedraogo, S.J., 2002. Millet production under pruned tree crowns in a parkland
456 system in Burkina Faso. *Agroforestry Sys.* 54(3), 203–214.

457 Baylis, G.T.S., 1950. Root system of the New Zealand mangrove. Transactions of the Royal Society of New
458 Zealand. 78, 509-514

459 Bell, J., & Lovelock, C. E. (2013). Insuring mangrove forests for their role in mitigating coastal erosion and
460 storm-surge: an Australian case study. *Wetlands*, 33(2), 279-289.

461 Berhongaray, G., Verlinden, M.S., Broeckx, L.S., Ceulemans, R., 2015. Changes in belowground biomass after
462 coppice in two *Populus* genotypes. *For. Eco. Man.* 337, 1-10.

463 Bischetti, G.B., Chiaradia, E.A., Epis, T., Morlotti, E., 2009. Root cohesion of forest species in the Italian Alps.
464 *Plant Soil* 324, 71-89.

465 Bischetti, G.B., Chiaradia, E.A., Simonato, T., Speziali, B., Vitali, B., Vullo, P., Zocco, A., 2005. Root strength
466 and root area of forest species in Lombardy. *Plant Soil* 278, 11-22.

467 Boldrin, D., Leung, A.K., Bengough, A.G., 2017. Root biomechanical properties during establishment of woody
468 perennials. *Ecol. Eng.* 109, 196-206.

469 Bordoloi, S., Ng, C.W.W., 2020. The effects of vegetation traits and their stability functions in bio-engineered
470 slopes: A perspective review. *Eng. Geology* 275, 105742.

471 Bordoni, M., Cislighi, A., Vercesi, A., et al., 2020. Effects of plant roots on soil shear strength and shallow
472 landslide proneness in an area of northern Italian Apennines. *Bull. Eng. Geol. Environ.* 79, 3361-3381.

473 Castañeda-Moya, E., Twilley, R.R., Rivera-Monroy, V.H., Marx, B.D., Coronado-Molina, C., Ewe, S.M.L.,
474 2011. Patterns of root dynamics in mangrove forests along environmental gradients in the Florida Coastal
475 Everglades USA. *Ecosys.* 14(7), 1178-1195.

476 Cellone, F., Carol, E., Tosi, L., 2016. Coastal erosion and loss of wetlands in the middle Río de la Plata estuary
477 (Argentina). *Applied Geography* 76, 37-48.

478 Chiaradia, E.A., Vergani, C., Bischetti, G.B., 2016. Evaluation of the effects of three European forest types on
479 slope stability by field and probabilistic analyses and their implications for forest management. *For. Eco.*
480 *Man.* 370, 114-129.

481 Chiatante, D., Scippa, G.S., Di Iorio, A., Sarnataro, M., 2003. The influence of steep slope on root system
482 development. *J. Plant Growth Regul.* 21, 247-260.

483 Cislaghi, A., 2018. Assessing shallow landslide susceptibility of vegetated hillslopes through a physically-based
484 spatially-distributed model (PhD dissertation in Environmental Sciences). Università degli Studi di
485 Milano, Milan, Italy.

486 Cislaghi, A., Alterio, E., Fogliata, P., Rizzi, A., Lingua, E., Vacchiano, G., Bischetti, G.B., Sitzia, T., 2021.
487 Effects of tree spacing and thinning on root reinforcement in mountain forests of the European Southern
488 Alps. *For. Ecol. Man.* 482, 118873.

489 Cohen, D., Schwarz, M., & Or, D. 2011. An analytical fiber bundle model for pullout mechanics of root
490 bundles. *J. Geophys. Res. Earth Surf.* 116, F3.

491 Danjon, F., Barker, D.H., Drexhage, M., Stokes, A., 2008. Using three-dimensional plant root architecture in
492 models of shallow-slope stability. *Ann. Bot.* 101, 1281-1293.

493 Das S, Crépin A.S., 2013. Mangroves can provide protection against wind damage during storms. *Estuar Coast*
494 *Shelf Sci* 134, 98-107.

495 Dazio, E., Conedera, M., Schwarz, M., 2018. Impact of different chestnut coppice managements on root
496 reinforcement and shallow landslide susceptibility. *For. Ecol. Man.* 417, 63-76.

497 De Baets, S., Poesen, J., Gyssels, G., Knapen, A., 2006. Effects of grass roots on the erodibility of topsoils
498 during concentrated flow. *Geomorphology* 76(1-2), 54-67.

499 De Baets, S., Poesen, J., Knapen, A., Galindo, P., 2007. Impact of root architecture on the erosion-reducing
500 potential of roots during concentrated flow. *Earth Surface Processes and Landforms*, 32(9), 1323-1345.

501 Dean, R.G., Galvin, C.J., 1976. Beach erosion: causes, processes, and remedial measures. *Critical Reviews Env.*
502 *Cont.* 6, 259-296.

503 Deljouei, A., 2019. Spatial dynamics of soil reinforcement due to presence of roots in Hyrcanian forest (Case
504 study: Kheyroud forest). (PhD dissertation in Forest Engineering). University of Tehran, Karaj, Iran.

505 Deljouei, A., Abdi, E., Schwarz, M., Majnounian, B., Sohrabi, H., Dumroese, R.K., 2020. Mechanical
506 characteristics of the fine roots of two broadleaved tree species from the temperate Caspian Hyrcanian
507 ecoregion. *Forests* 11, 345.

508 Demenois, J., Rey, F., Stokes, A., Carriconde, F., 2017. Does arbuscular and ectomycorrhizal fungal inoculation
509 improve soil aggregate stability? A case study on three tropical species growing in ultramafic Ferralsols.
510 *Pedobiologia* 64, 8-14.

511 Di Iorio, A., Lasserre, B., Scippa, G.S., Chiatante, D., 2005. Root system architecture of *Quercus pubescens*
512 trees growing on different sloping conditions. *Ann. Bot.* 95, 351–361.

513 Docker, B.B., Hubble, T.C.T., 2008. Quantifying root-reinforcement of river bank soils by four Australian tree
514 species. *Geomorphology* 100(3-4), 401-418.

515 Fan, C.C., Su, C.F., 2009. Effect of soil moisture content on the deformation behaviour of root-reinforced soils
516 subjected to shear. *Plant Soil* 324, 57-69.

517 Feagin, R.A., Furman, M., Salgado, K., Martinez, M.L., Innocenti, R.A., Eubanks, K., Figlus, J., Huff, T.P.,
518 Sigren, J., Silva, R., 2019. The role of beach and sand dune vegetation in mediating wave run up erosion,
519 *Estuarine. Coastal Shelf Sci.* 219, 97-106.

520 Feagin, R.A., Irish, J., Möller, I., Williams, A., Colón-Rivera, R., Mousavi, M., 2011. Short communication:
521 engineering properties of wetland plants with application to wave attenuation. *Coast Eng.* 58, 251-255.

522 Fortier, J., Truax, B., Gagnon, D., Lambert, F., 2013. Root biomass and soil carbon distribution in hybrid poplar
523 riparian buffers, herbaceous riparian buffers and natural riparian woodlots on farmland. *Springer Plus*
524 DOI: 10.1186/2193-1801-2-539.

525 Ganatsas, P., Spanos, P., 2005. Root system asymmetry of Mediterranean pines. *Plant Soil* 278, 75-83.

526 Gedan, K.B., Kirwan, M.L., Wolanski, E., Barbier, E.B., Silliman, B.R., 2011. The present and future role of
527 coastal wetland vegetation in protecting shorelines: answering recent challenges to the paradigm.
528 *Climatic Change* 106(1), 7-29.

529 Genet, M., Stokes, A., Fourcaud, T., Hu, X., Lu, Y., 2006. Soil fixation by tree roots: changes in root
530 reinforcement parameters with age in *Cryptomeria japonica* D. Don. plantations. In *Interpraevent*, pp.
531 535–542.

532 Genet, M., Stokes, A., Fourcoud, T., Norris, J.E., 2010. The influence of plant diversity on slope stability in a
533 moist evergreen deciduous forest. *Ecol. Eng.* 36, 265-275.

534 Genet, M., Stokes, A., Salin, F., Mickovski, S.B., Fourcaud, T., Dumail, J.F., van Beek, R., 2005. The influence
535 of cellulose content on tensile strength in tree roots. *Plant Soil*, 278, 1-9.

536 Ghestem, M., Cao, K., Ma, W., Rowe, N., Leclerc, R., Gadenner, C., Stokes, A., 2014. A framework for
537 identifying plant species to be used as “Ecological Engineers” for fixing soil on unstable slopes. *Plos One*
538 DOI: 10.1371/journal.pone.0095876.

539 Giadrossich, F., Cohen, D., Schwarz, M., Seddaiu, G., Contrain, N., Lubino, M., Valdes-Rodriguez, O.A.,
540 Niedd, M., 2016. Modelling bio-engineering traits of *Jatropha curcas* L. *Ecol. Eng.* 89, 40-48.

541 Giadrossich, F., Schwarz, M., Cohen, D., Cislazhi, A., Vergani, C., Hubble, T., Phillips, C., Stokes, A., 2017.
542 Methods to measure the mechanical behavior of tree roots: a review. *Ecol. Eng.* 109, 256-271.

543 Gysse, G., Poesen, J., Bochet, E., Li, Y., 2005. Impact of plant roots on the resistance of soils to erosion by
544 water: a review. *Prog. Phys. Geogr.* 29, 189-217.

545 Hales, T.C., Ford, C.R., Hwang, T., Vose, J.M., Band, L.E., 2009. Topographic and ecologic controls on root
546 reinforcement. *J. Geophys. Res.* 114, <https://doi.org/10.1029/2008JF001168>

547 Hales, T.C., Miniati, C.F., 2017. Soil moisture causes dynamic adjustments to root reinforcement that reduce
548 slope stability. *Earth Surf. Process. Landforms* 42, 803–813. est area play a significant role in reducing
549 soil erosion and conservation of nutrient levels in the mangrove forest.

550 Hamidifar, H., Keshavarzi, A., Truong, P., 2018. Enhancement of river bank shear strength parameters using
551 Vetiver grass root system. *Arab. J. Geosci.* 11, 611, doi:10.1007/s12517-018-3999-z

552 Hoad, S.P., Russell, G., Lucas, M.E., Bingham, I.J., 2001. The management of wheat, barley, and oat root
553 systems. *Adv. Agronomy* 74, 193-247.

554 Hudek, C., Stanchi, S., D’Amico, M., Freppaz, M., 2017. Quantifying the contribution of the root system of
555 alpine vegetation in the soil aggregate stability of moraine. *Int. Soil Water Conserv. Res.* 5, 36-42.

556 Jackson, R.B., Canadell, J., Ehleringer, J.R., Mooney, H.A., Sala, O.E., Schulze, E.D., 1996. A global analysis
557 of root distributions for terrestrial biomes. *Oecologia* 108, 389-411.

558 Ji, J., Kokutse, N., Genet, M., Fourcaud, T., Zhang, Z., 2012. Effect of spatial variation of tree root
559 characteristics on slope stability. A case study on Black Locust (*Robinia pseudoacacia*) and Arborvitae
560 (*Platycladus orientalis*) stands on the Loess Plateau, China. *Catena*, 92, 139-154.

561 Khodadadi-Jokari, K., 2003. The Final Report on Hydrobiology of Laft and Khamir (Khooran Estuaries),
562 Hormozgan Province. Project No. 83/757. Persian Gulf and Oman Sea Ecology Research Center,
563 Ecology Department, Iran.

564 Leung, F.T.Y., Yan, W.M., Hau, B.C.H., Tham, L.G., 2015. Root systems of native shrubs and trees in Hong
565 Kong and their effects on enhancing slope stability. *Catena*, 125, 102-110.

566 Li, Z.W., Zhang, G.H., Geng, R., Wang, H., Zhang, X.C., 2015. Land use impacts on soil detachment capacity
567 by overland flow in the Loess Plateau, China. *Catena*, 124, 9-17.

568 Löbmann, M.T., Tonin, R., Wellstein, C., Zerbe, S., 2020. Determination of the surface-mat effect of grassland
569 slopes as a measure for shallow slope stability. *Catena*, 187, 104397.

570 Mamo, M., Bubenzer, G.D., 2001a. Detachment rate, soil erodibility and soil strength as influenced by living
571 plant roots: Part II. Field study. *American Soc. Agr. Eng.* 44, 1175-1181.

572 Mamo, M., Bubenzer, G.D., 2001b. Detachment rate, soil erodibility and soil strength as influenced by living
573 plant roots: Part I. Laboratory study. *American Soc. Agr. Eng.* 44, 1167-1174

574 Mao, Z., Saint-André, L., Genet, M., Mine, F.-X., Jourdan, C., Rey, H., Courbaud, B., Stokes, A., 2012.
575 Engineering ecological protection against landslides in diverse mountain forests: Choosing cohesion
576 models. *Ecol. Eng.* 45, 55-69.

577 Marler, T.E., Discekici, H.M., 1997. Root development of “Red Lady” papaya plants grown on a hillside. *Plant*
578 *Soil* 195, 37–42.

579 Mazda Y, Magi M, Nanao H, Kogo M, Miyagi T, Kanazawa N, Kobashi D (2002) Coastal erosion due to long-
580 term human impact on mangrove forests. *Wetl Ecol Manag* 10:1-9.

581 McKee, K.L., Cahoon, D.R., Feller, I.C., 2007. Caribbean mangroves adjust to rising sea level through biotic
582 controls on change in soil elevation. *Global Eco. Biogeography* 16, 545-556.

583 Mehtab, A., Jiang, Y. J., Su, L. J., Shamsher, S., Li, J. J., Mahfuzur, R., 2021. Scaling the Roots Mechanical
584 Reinforcement in Plantation of *Cunninghamia* R. Br in Southwest China. *Forests*, 12(1), 33.

585 Mitra, A., 2020. *Mangrove Forests in India, Exploring Ecosystem Services*. Springer International Publishing
586 A.G.: Cham, Switzerland, 353 p.

587 Mohammadizadeh, M., Farshchi, P., Danehkar, A., Mahmoodi-Madjdabadi, M., Hassani, M.,
588 Mohammadizadeh, F., 2009. Interactive effect of planting distance, irrigation type and intertidal zone on
589 the growth of grey mangrove seedlings in Qeshm island, Iran. *J. Trop. Forest Sci.* 21, 147-155.

590 Montagnoli, A., Terzaghi, M., Di Iorio, A., Scippa, G.S., Chiatante, D., 2012. Fine-root seasonal pattern,
591 production and turnover rate of European beech (*Fagus sylvatica* L.) stands in Italy Prealps: possible
592 implications of coppice conversion to high forest. *Plant Biosystems.* 146(4), 1012-1022.

593 Moresi, F.V., Maesano, M., Matteucci, G., Romagnoli, M., Sidle, R.C., Scarascia Mugnozza, G., 2019. Root
594 biomechanical traits in a montane Mediterranean forest watershed: Variations with species diversity and
595 soil depth. *Forests* 10, 341.

596 Ni, J.J., Leung, A.K., Ng, C.W.W., Shao, W., 2018. Modelling hydro-mechanical reinforcements of plants to
597 slope stability. *Computers Geotech.* 95, 99-109.

598 Nguyen, H.T.L., and Luong, H.P.V. 2019. Erosion and deposition processes from field experiments of
599 hydrodynamics in the coastal mangrove area of Can Gio, Vietnam. *Oceanologia.* 61, 252-264.

600 Odhiambo, H.O., Ong, C.K., Douglas, J.D., Wilson, J., Khan, A.A.H., Sprent, J.I., 2001. Roots, soil water and
601 crop yield: tree crop interactions in a semi-arid agroforestry system in Kenya. *Plant Soil* 235, 221-233.

602 Operstein, V., Frydman, S., 2000. The influence of vegetation on soil strength. *Proc. Inst. Civ. Eng. Ground*
603 *Improv.* 4, 81-89.

604 Osman, N., Barakbah, S.S., 2011. The effect of plant succession on slope stability. *Ecol. Eng.* 37, 139-147.

605 Othman M.A., 1994. Value of mangroves in coastal protection. *Hydrobiologia* 285, 277-282.

606 Pandey, C.B., Singh, A.K., Sharma, D.K., 2000. Soil properties under *Acacia nilotica* trees in a traditional
607 agroforestry system in central India. *Agroforestry Sys.* 49, 53-61.

608 Pollen, N., 2008. Temporal and spatial variability of root reinforcement in stream banks: Accounting for soil
609 shear strength and moisture. *Catena* 69, 197-205.

610 Pollen, N., Simon, A., 2005. Estimating the mechanical effects of riparian vegetation on stream bank stability
611 using a fiber bundle model. *Water Resour. Res.* 41, W07025, doi:10.1029/2004WR003801.

612 Pongpam, S., Charoenphonphakdi, T., Sangtiew, T., Patanaponpaiboon, P., 2016. Fine root production in three
613 zones of secondary mangrove forest in eastern Thailand. *Trees Struc. Func.* 30(2), 467-474.

- 614 Preti, F., 2006. Stabilit' a dei versanti vegetati, Cap. 10, in: Manuale 3 d'Ingegneria Naturalistica Sistemazione
615 dei versanti, edited by: Sauli, G., Cornellini, P., Preti, F., Regione Lazio, Roma, pp. 137-168.
- 616 Rezaii, Y., 1993. Study on pharmacognosy effect of *Avicennia marina*. PhD thesis, Pharmaceutics Collage
617 Tehran University of Medical Sciences, Tehran, Iran.
- 618 Rippey, E., Rowland, B., 2004. Coastal plants: Perth and the south-west region (2nd ed.). Perth: UWA Press
619 (University of Western Australia Press).
- 620 Safiari, S., 2003. Mangrove forests; Mangrove forests of Iran. Publication of Research Institute of Forests and
621 Rangelands of Iran, No. 314, Tehran, vol 2, 539p (In Persian).
- 622 Sagheb-Talebi, K., Sajedi, T., Pourhashemi, M., 2014. Forests of Iran: a treasure from the Past, a Hope for the
623 Future, Springer.
- 624 Sánchez, B.G., 2005. Belowground productivity of mangrove forests. Dissertation, (December).
- 625 Schwarz, M., Cohen, D., Or, D., 2010b. Root-soil mechanical interactions during pullout and failure of root
626 bundles. J. Geophys. Res. 115, F4.
- 627 Schwarz, M., Giadrossich, F., Cohen D., 2013. Modeling root reinforcement using a root failure Weibull
628 survival function. Hydrol. Earth. Syst. Sci. 17, 4367-4377.
- 629 Schwarz, M., Preti, F., Giadrossich, F., Lehmann, P., Or, D., 2010a. Quantifying the role of vegetation in slope
630 stability: A case study in Tuscany (Italy). Ecol. Eng. 36, 285-291.
- 631 Schwarz, M., Rist, A., Cohen, D., Giadrossich, F., Egorov, P., Büttner, D., Stolz, M., Thormann, J.J., 2015.
632 Root reinforcement of soils under compression. J. Geophysical Res. Earth Surf. 120, 2103-2120.
- 633 Shepard, C.C., Crain, C.M., Beck, M.W., 2011. The protective role of coastal marshes: a systematic review and
634 meta-analysis. Plos One 6, e27374.
- 635 Sidle, R.C., Bogaard, T.A., 2016. Dynamic earth system and ecological controls of rainfall-initiated landslides.
636 Earth-Sci. Rev. 159, 275-291.
- 637 Sidle, R.C., Ochiai, H., 2006. Landslides: processes, prediction and land use. American Geophysical Union
638 (AGU), 2000 Florida Avenue N.W., Washington, D.C. 20009-1277, USA. Water Resources Monograph,
639 312 p.
- 640 Smee, D.L., 2019. Coastal ecology: living shorelines reduce coastal erosion. Current Biol. 29, 411-413.

641 Stokes, A., Atger, C., Bengough, A.G., Fourcaud, T., Sidle, R.C., 2009. Desirable plant root traits for protecting
642 natural and engineered slopes against landslides. *Plant Soil* 324, 1-30.

643 Thampanya, U., Vermaat, J. E., Sinsakul, S., & Panapitukkul, N. (2006). Coastal erosion and mangrove
644 progradation of Southern Thailand. *Estuarine, coastal and shelf science*, 68(1-2), 75-85.

645 Thompson, B.S., Primavera, J.H., Friess, D.A., 2017. Governance and implementation challenges for Mangrove
646 forest payments for ecosystem services (PES): empirical evidence from the Philippines. *Ecosyst. Serv.*
647 23, 146-155.

648 Van Rijn, L.C., 2011. Coastal erosion and control. *Ocean Coast. Manag.* 54, 867-887.

649 Van Tang, T., Rene, E. R., Binh, T. N., Behera, S. K., & Phong, N. T. (2020). Mangroves diversity and erosion
650 mitigation performance in a low salinity soil area: case study of Vinh City, Vietnam. *Wetlands Ecology*
651 *and Management*, 28(1), 163-176.

652 Vannoppen, W., De Baets, S., Keeble, J., Dong, Y., Poesen, J., 2017. How do root and soil characteristics affect
653 the erosion-reducing potential of plant species?, *Ecol. Eng.* 109(B), 186-195.

654 Vergani, C., 2013. Spatial and temporal dynamics of root reinforcement in Alpine forests. PhD thesis.
655 University Degli Studi Di Milano, 194 p.

656 Vergani, C., Chiaradia, E.A., Bischetti, G.B., 2012. Variability in the tensile resistance of roots in Alpine forest
657 tree species. *Ecol. Eng.* 46, 43-56.

658 Waldron, L.J., 1977. The shear resistance of root-permeated homogeneous and stratified soil. *Soil Sci. Soc.*
659 *America J.* 41, 843-849.

660 Wu, T.H., 1976. Investigation on landslides on Prince of Wales Island, Alaska. *Geotech Rpt. No 5*, Dpt. of Civil
661 Engineering, Ohio State University, Columbus, USA.

662 Wu, T.H., 1995. Slope stabilization. *Slope Stab. Eros. Control Bioeng. Approach* 233, 221-264.

663 Wu, T.H., McKinnell, W.P., Swantson, D.N., 1979. Strength of tree roots and landslides on Prince of Wales
664 Island, Alaska. *Canadian Geotechnical. J.* 16, 19-33.

665 Wu, T.H., McOmber, R.M., Erb, R.T., Beal, P.E., 1988. Study of soil-root interaction. *J. Geotechnical. Eng.*
666 114, 1351-1375.

- 667 Yang, Y., Wang, J., Duan, Q., Su., C., Yan, M., Dong, Y., 2018 The investigation and 3D numerical simulation
668 of herb roots in reinforcing soil and stabilizing slope. KSCE. J. Civ. Eng. 22, 4909-4921.
- 669 Ye, C., Guo, Z., Li, Z., Cai, C., 2017. The effect of Bahiagrass roots on soil erosion resistance of Aquults in
670 subtropical China. Geomorphology 285, 82-93.